Maritime Technology and Research

https://so04.tci-thaijo.org/index.php/MTR

Research Article

A novel vortex-induced vibration-based piezoelectric powered generator for maritime propulsion systems

Sirawit Shimpalee[1], Vijay Sethuraman[2], Michelle Spigner[1] and Sirivatch Shimpalee[2,*]

[1]*Spring Valley High School, Columbia, SC 29229, USA*
[2]*Department of Chemical Engineering, University of South Carolina, Columbia, SC 29208, USA*

Article information
Received: April 13, 2020
Revised: May 18, 2020
Accepted: June 5, 2020

Keywords
Vortex Induced Vibration,
Piezoelectric,
Vortex shedding,
Spring constant

Abstract

Vortex Induced Vibrations (VIVs), a phenomenon where fluid flow causes oscillations against an object called a bluff body by vortex shedding, have been studied as a source of renewable energy. However, few studies have focused on the use of VIVs for maritime propulsion. In this investigation, a novel VIV-based piezoelectric generator and rechargeable battery were created for use as a maritime propulsion system. The purpose of this research was to see if piezoelectricity is a feasible source of power for a maritime propulsion system. It was hypothesized that, if different velocities are applied to a piezoelectric generator, then 3.4 m/s would produce the most power to operate a model ship. In order to determine the feasibility of the generator, testing was conducted in stages, where each stage saw different modifications to the generator. Each generator design was then exposed to 8 different velocities. Afterwards, the data was analyzed through the use of line graphs, box plots, and ANOVAs. It was determined that, although the hypothesis was partially supported in some cases, it was ultimately not supported due to the behavior of the most powerful configuration. Furthermore, the ANOVA tests determined that $p < \alpha$, meaning that significant differences existed between frequencies as a result of velocity and spring constant, while the number of piezoelectric transducers and velocity affected the voltage. No combination achieved enough output to sufficiently operate a model ship. However, the effectiveness of the generator can be improved by implementing an efficient circuit and modification of the transducers.

1. Introduction

Oscillations, including vortex-induced vibrations (VIVs), have been recently studied as a source of renewable energy. However, VIVs are distinguished from other oscillations in that the extent of the oscillations are dependent on fluid velocity. VIV occurs when the inconsistent viscosity of fluid flow causes the formation of vortices in different locations, but in an alternating pattern (Shimpalee, 2019). This is called vortex shedding. At certain velocities, the rate of vortex shedding caused by fluid flow coincides with the forming oscillations of the bluff body, allowing for the lock-in phenomenon and the highest amplitudes to occur. Because of this unique behavior, VIVs have been studied for many uses, with some of the more notable ones being related to maritime studies. Energy from VIVs can be harvested using many different methods. Mechanical

[*]*Corresponding author: Department of Chemical Engineering, University of South Carolina, Columbia, USA*
E-mail address: shimpale@cec.sc.edu

methods, however, can suffer from high energy loss and friction (Shimpalee, 2019). As a result, electrical methods, such as piezoelectric generators, are preferred (Shimpalee, 2019). Piezoelectricity refers to the ability of certain materials to generate an electric potential when exposed to vibrations and other forms of mechanical stress. This electric potential is converted and harvested through the use of electrodes. In this investigation, a novel VIV-based piezoelectric generator and rechargeable battery were created for use as a maritime propulsion system.

The source of power of piezoelectric generators comes from fluid flow. When a VIV system is exposed to a certain velocity, the lock-in phenomenon occurs, allowing for oscillations with the highest amplitudes to occur. Thus, different velocities were applied to observe changes in the performance of the generator. However, in order to understand how these oscillations affect piezoelectricity, one must understand how a generator functions. A piezoelectric generator is made up of the piezoelectric element, dampers, and springs (Jbaily & Yeung, 2014), a setup which is similar to that of a VIV generator. Of the piezoelectric materials used in generators, Lead Zirconate Titanate (PZT) and Polyvinylidene Fluoride (PVDF) are used most frequently in maritime settings (Jbaily & Yeung, 2014). Each material has its benefits and downsides, with PZT being more powerful but fragile than PVDF. When oscillations are introduced, the piezoelectric material is put under stress, resulting in voltage generation (Jbaily & Yeung, 2014). However, the largest oscillations do not result in the highest power output (Mehmood et al., 2013). Furthermore, the setup of a generator affects the optimal velocities, with the optimal range, as described by Dai et al. (2016), of 3.0 to 4.4 m/s being significantly different from the 1.4 to 1.6 m/s range of previous research (Shimpalee, 2019). These results are also impacted by damping; Franzini and Bunzel (2018) found that adding another set of dampers increased the output of their generator from 2.6 to 11 MW. As a result, the lock-in phenomenon did not offer the best indication of efficiency, and tests were carried out without total reliance on the aforementioned phenomenon.

The amount of power and potential that was generated from the VIVs was measured, since they are the most important aspects of the generator. Although vibrations are the main source of power for piezoelectric generators, the components of the electrical circuit are what allow the power of the generator to be usable. Electrodes, which are devices designed to transfer electrical currents from non-metallic solids, first capture the generated charges. The potential is then captured by a transformer. The activities of the 2 aforementioned components, which constitute the mechanical portion of the generator, generate the charges of the electrical converters (Jbaily & Yeung, 2014). However, AC current is generated, not the DC required for other electrical appliances. As a result, the current is processed and converted through the use of a rectifier bridge that includes a filtering capacitor (Jbaily & Yeung, 2014). This power can then be used as a charger for a rechargeable battery. Changes to the specific set-up of generators and their environments result in different capabilities. Martinez et al. (2019) utilized a longitudinal traveling wave transformer and were able to achieve 6.5 W and 90 % efficiency for their generator. As for VIV-based generators, Jbaily & Yeung (2014) observed and found that the power output ranged from 6.81×10^{-6} to 0.004 W. They also found that the power density was 11 to 68 W/m^3 and the efficiency was 11 to 37 %. The aforementioned results are due to different compositions of the circuits. For example, increasing the load resistance also increased the power (Zhang & Wang, 2016), thus improving the generator. This information was taken into account for this work during the creation of the piezoelectric generator.

The purpose of this research was to see if piezoelectricity is a feasible source of power for a maritime propulsion system through the optimization of velocity and spring combinations. This was done as an extension of previous research on VIV-based maritime propulsion systems. Mechanical methods are not efficient in creating a reliable maritime propulsion system, but an indirect system that involves a battery opens up many possibilities for research that is relatively new (Shimpalee, 2019). In addition, piezoelectricity was also accessible to the researchers, allowing for the appropriate conduction of the proposed research. Potential benefits of this research include reducing existing costs for maritime propulsion systems, as well as providing a new common source of

energy to replace non-renewable resources. For this research, a piezoelectric generator was created. This generator was then exposed to several different velocities. The oscillations from the generator produced output in the form of potential (V) and power (MW), which would be applicable to both the rechargeable battery and the piezoelectric material. This output was measured using an oscilloscope and multimeter, then analyzed using ANOVAs, line graphs, and box plots. Two stages were included in this research, but the main hypothesis was that if different velocities were applied to a piezoelectric generator, then a generator utilizing 2 transducers with 54 N/m springs running at 3.4 m/s would produce the most power to operate a model ship.

2. Materials and methods

A generator was created in order to conduct the research. The design of this generator was chosen based on previous research and the notion of consistency with other papers in the relevant field. PVC pipes constituted the main framework of the generator. The vertical supports of the frame were 32.95 cm in length, while the horizontal supports were 25.20 cm. Between these supports a 2.75 cm bluff body with a mass of 85 g was placed, using one of the following spring constants: 205, 636, 93, 152, 314, and 54 N/m. This particular bluff body and set of springs was selected due to being the most optimal for the structure based on its dimensions. To support the bluff body and dampers, brass hooks were attached to these horizontal supports. These hooks were 3.45 cm away from the edge of the PVC pipe. To prevent the design from falling over, pipes were attached to the T-connectors, with PVC pipes added to increase their effectiveness. This base resembled an “H” when viewed from above. The frame was then attached to a plywood board with bolts for further support and to provide a base for the piezoelectric circuit.

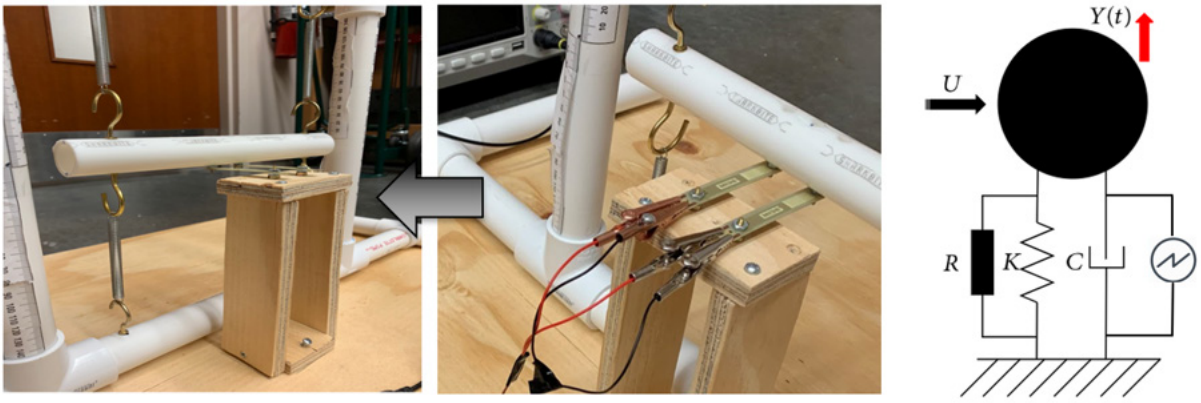

Figure 1 The design of the piezoelectric generator when 2 transducers are used. A wooden structure was the most practical design for the generator. The structure was determined not to interfere with the actual vortex shedding. The middle component shows a close up of the transducers with portions of the oscilloscope. To the right is an electrical diagram showing the circuit setup of the experimentation.

Figure 1 presents the actual design of the generator. A rectangular structure was created to incorporate a piezoelectric system into the vortex induced vibrations (VIVs) used. The rectangular structure was constructed out of plywood and placed in front of the bluff body. This placement was done in order to prevent interference with the vortex shedding, which is the main source of oscillations during VIVs. This location was also selected due to the lack of feasibility of placing the piezoelectric transducers on the hooks and springs. On the top of the structure, Mide Corp. Piezoelectric Bending Transducers were placed and attached. These transducers were selected because they were the most compatible with the behavior of the bluff body, particularly the

amplitude. The transducers were attached to the bluff body using nuts and bolts, which was possible through holes already existing in the design of the transducer. Meanwhile, the copper end of the transducer was placed on the rectangular structure, which allowed for the attachment of clips, depending on which stage of testing the generator was undergoing. This equipment was obtained from several locations. **Figure 1** also displays a circuit diagram of the experimental setup, where the resistor, spring, and capacitor represent components of the transducer. The diagram also shows the transducer attached to the oscilloscope.

The capabilities of the generator were tested by exposing it to the following velocities: 1.0, 1.4, 1.6, 2.0, 2.4, 2.7, 3.0, and 3.4 m/s. The velocities were produced using a Pelonis™ 50.8 cm fan and modifying the distance between the fan and the generator. An anemometer was used to confirm the velocities. While the generator was exposed to the fluid flow, a Siglent® SDS1202X-E oscilloscope recorded the behavior of the power production by attaching clips between the transducer and the device. The data was presented on the oscilloscope in the form of a wave function line graph, displaying the peaks of power over time. This data was then recorded using a USB drive and uploaded to a computer for analysis. Each test took 30 min to run. This time interval, as well as the fluid used, bluff body diameter and mass, and structural design parameters were controlled. The experimentation consisted of 2 stages. The first stage consisted of recording the potential (V) and frequency (Hz) of one transducer for all 6 springs. The second stage selected 2 springs that produced the highest average potential. The springs were then used with 2 piezoelectric transducers connected in series, tested, and compared with configurations utilizing only one transducer.

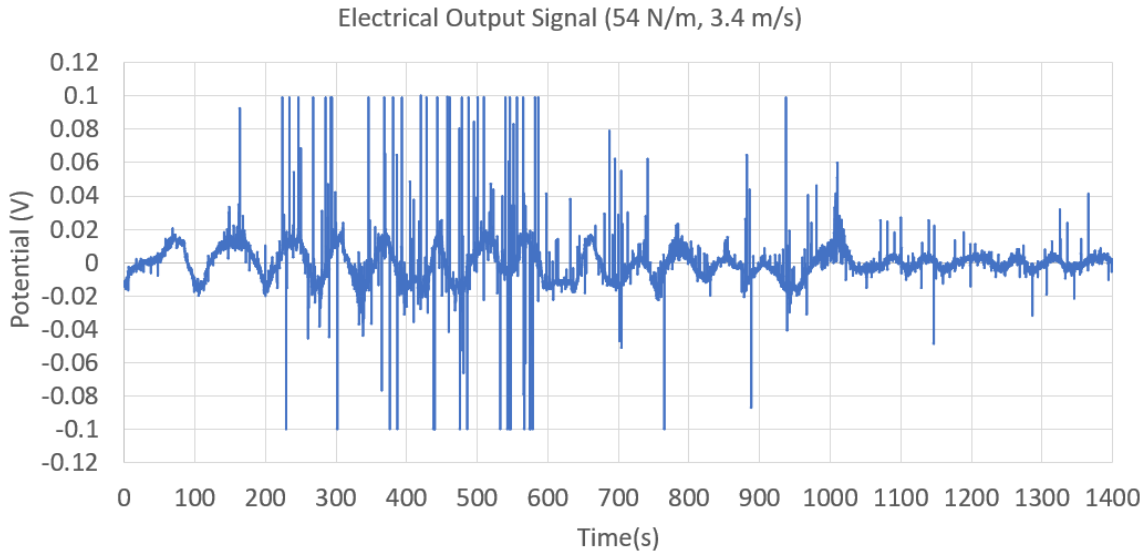

Figure 2 The electrical output signal for the generator with a 54 N/m spring, one transducer, running at 3.4 m/s combination. Because of the nature of the data, the results were processed and analyzed into a more legible and understandable form.

Power was analyzed using Microsoft® Excel for descriptive statistics and SigmaPlot® for inferential statistics. An example of the data received from the oscilloscope is seen in **Figure 2**. Noise is observed in the figure, likely due to interference from the testing environment. Because of the format, the data was processed and summarized. Data for each trial was summarized into 2 categories for descriptive statistics: average frequency and average amplitude of potential. After that, the overall behavior of the power for the 2 stages was graphed for a visual representation using line graphs. For inferential statistics, significant differences between the voltages through velocity, spring constant, and the number of piezoelectric transducers were analyzed using multiple-way

analysis of variance (ANOVA) tests. These tests were used in order to determine any realistic differences between velocities for real world use. The ANOVA tests were conducted using the data described in the descriptive statistics. Holm-Sidak tests, which correct errors for multiple comparisons, were used for post hoc analysis. This data determined the feasibility of scaling up.

3. Results

Table 1 displays the averages of output (V) amplitudes for the 6 springs tested in relation to velocity. Based on the data, the 205 N/m spring achieved the highest average of 0.065647 V at 3.4 m/s. The overall amplitude values were followed by the 93 N/m spring, with the 54 N/m spring achieving the lowest amplitudes. Based on the results, the 205 and 93 N/m were used for **Tables 3** and **4**, as well as **Figures 5** and **6**.

Table 1 A comparison of spring constant and potential (V) of one piezoelectric transducer in relation to velocity.

Velocity (m/s)	54 N/m	93 N/m	152 N/m	205 N/m	314 N/m	636 N/m
1.0	0.017358	0.008659	0.005583	0.000852	0.006064	0.004889
1.4	0.031516	0.002290	0.000698	0.005997	0.002053	0.000763
1.6	0.002330	0.042263	0.008814	0.016168	0.001664	0.001687
2.0	0.002347	0.032316	0.001159	0.055424	0.002539	0.025976
2.4	0.002828	0.060425	0.034294	0.017375	0.024241	0.037524
2.7	0.002770	0.061048	0.003071	0.044202	0.035470	0.027952
3.0	0.003774	0.004696	0.039971	0.061084	0.004128	0.004637
3.4	0.007316	0.008096	0.044383	0.065647	0.057116	0.055509

This table shows the average amplitudes of potential of velocity for each spring constant and velocity combination. The 205 and 93 N/m springs achieved the highest amplitudes overall, while the 54 N/m output values were the lowest, followed by the 636 N/m spring.

Table 2 shows the frequencies of the potential behavior for each spring with respect to velocity. A major difference did not exist between all springs, with the largest difference existing between the 93 and 636 N/m springs. The overall frequency of the springs tended to be within the range of 2.0 to 4.2 Hz. This means that frequency is relatively insignificant when considering the use of one piezoelectric transducer.

Table 2 A comparison of spring constant and frequency (Hz) of one piezoelectric transducer in relation to velocity.

Velocity (m/s)	54 N/m	93 N/m	152 N/m	205 N/m	314 N/m	636 N/m
1.0	3.5	3.6	2.9	3.5	3.1	3.1
1.4	3.4	3.4	3.8	3.5	3.6	3.3
1.6	3.6	4.1	3.0	3.7	4.0	3.7
2.0	3.6	4.2	3.7	3.8	3.6	2.6
2.4	3.1	4.0	2.9	3.3	3.3	2.4
2.7	3.5	3.8	3.2	2.8	3.3	2.6
3.0	3.7	2.8	3.4	3.1	3.3	3.1
3.4	3.4	3.6	3.0	3.2	3.3	2.0

This table shows the frequencies as a result of spring constant and velocity. The frequencies were within approximately 2.0 Hz from each other, meaning that the tables indicate a lack of difference. ANOVAs would be needed to confirm or refute this.

Table 3 A comparison of potential (V) of one and 2 piezoelectric transducers for 2 spring constants in relation to velocity.

Velocity (m/s)	93 N/m 1 piezo	205 N/m 1 piezo	93 N/m 2 piezo	205 N/m 2 piezo
1.0	0.008659	0.000852	0.054637	0.054890
1.4	0.002290	0.005997	0.061394	0.062275
1.6	0.042263	0.016168	0.056881	0.072819
2.0	0.032316	0.055424	0.134213	0.049218
2.4	0.060425	0.017375	0.141151	0.053925
2.7	0.061048	0.044202	0.242275	0.224070
3.0	0.004696	0.061084	0.081597	0.224695
3.4	0.008096	0.065647	0.081966	0.225380

This table shows the effect that the addition of another transducer has on potential. Two piezoelectric transducers result in more output. This trend is not for all velocities. However, overall, more velocities display more output for more transducers than those that do not.

Table 3 reflects upon the potential of one and 2 piezoelectric transducers for the 93 and 205 N/m springs as a result of velocity. The aforementioned springs were selected since they achieved the highest average potential amplitudes. Based on the results, the 2 transducer combinations produced potentials around 3 times greater than one piezo for most of the velocities used, except at velocities between 2.0 and 2.4 m/s. This means that using multiple piezoelectric transducers affects the potential produced.

Table 4 shows the frequency values that came from the testing conditions seen in **Table 3**. The differences between the frequencies are increased, with differences of up to twice as much. However, the 93 N/m spring constant with 2 piezoelectric transducers had a higher frequency than one transducer at 1.4 and 3.0 m/s. In addition, this must be taken in context with the amplitudes seen in **Table 3**. As a result, the amplitudes of the 2 transducer combinations more than compensates for the frequency, which means that there exists a difference of output when regarding the number of piezoelectric transducers.

Table 4 A comparison of frequency (Hz) of one and 2 piezoelectric transducers for 2 spring constants in relation to velocity.

Velocity (m/s)	93 N/m 1 piezo	205 N/m 1 piezo	93 N/m 2 piezo	205 N/m 2 piezo
1.0	3.6	3.5	1.7	1.8
1.4	3.4	3.5	3.7	1.6
1.6	4.1	3.7	3.4	1.8
2.0	4.2	3.8	3.5	2.1
2.4	4.0	3.3	1.6	2.1
2.7	3.8	2.8	1.5	2.2
3.0	2.8	3.1	3.6	2.2
3.4	3.6	3.2	3.4	2.1

This table shows the values for frequency when comparing the difference another transducer makes on the system. Although the addition of another transducer reduces frequency for many cases, some velocities and combinations, such as at 1.4 m/s for the 93 N/m spring, result in a higher frequency.

Figure 3 shows the behavioral trends of amplitude of potential in relation to velocity for each spring constant. Based on the graph, there is no standard lock-in region for all springs except the 54 N/m spring. The 93 N/m spring had several peaks in behavior, while the 205, 314, and 636 N/m behaviors plateaued to amplitudes higher than those achieved with the lock-in phenomenon. The 152 N/m spring experienced both trends. In addition, springs with relatively extreme spring constants had lower outputs than non-extreme values.

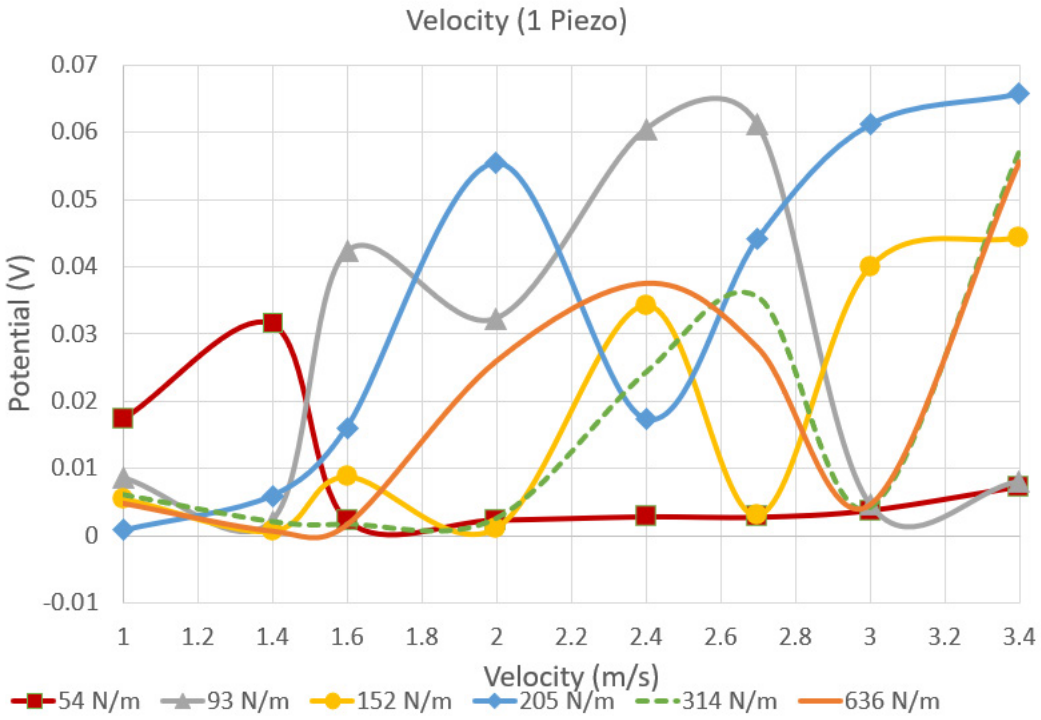

Figure 3 Behavioral trends of potential amplitude in relation to velocity for each spring constant. This graph shows a comparison of different spring constants (N/m) on the potential (V) in relation to velocity (m/s). The highest potential values were achieved when the spring constant was 205 or 93 N/m.

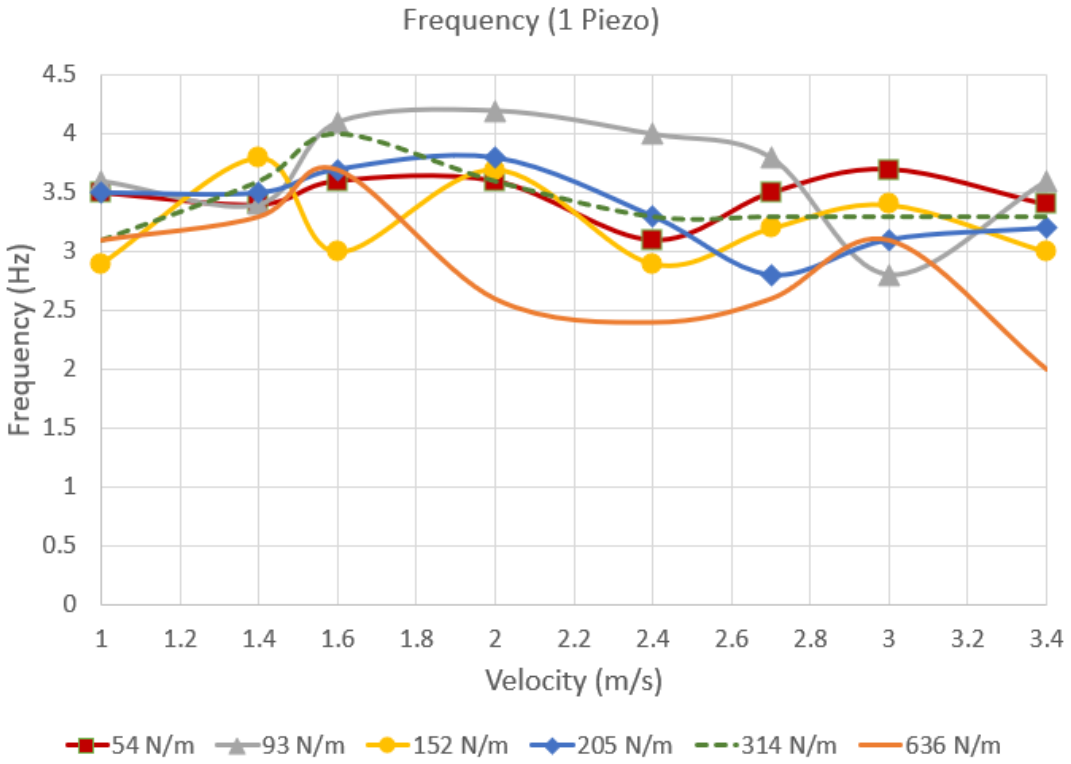

Figure 4 Behavioral trends for frequency in relation to velocity for each spring constant. This graph shows the general trend of frequency (Hz) for different spring constants (N/m) in relation to velocity (m/s) for one piezoelectric transducer. Overall, the frequency is relatively constant, with a slight negative correlation. The difference is marginal overall.

Figure 4 elaborates on the behavior of the frequency of potential in relation to velocity for each spring constant. This figure corroborates the results from **Table 2**. Similar to the related table, the frequency of each setup tended to stay the same overall, with a slight negative correlation. The most deviation started to occur from 1.4 m/s. However, the figure helps to better define the differences between each spring, which was important in determining the actual power output of each combination.

Figure 5 visualizes the relationship of potential amplitude, velocity, and the number of transducers for the 93 and 205 N/m springs. Based on the trends shown, the addition of another transducer greatly increased the potential for most velocities. Furthermore, the behavior of the 2 transducer graphs seems to be similar to the trends of the one transducer graphs for each respective spring. This figure must be taken with respect to **Figure 6** for output differences.

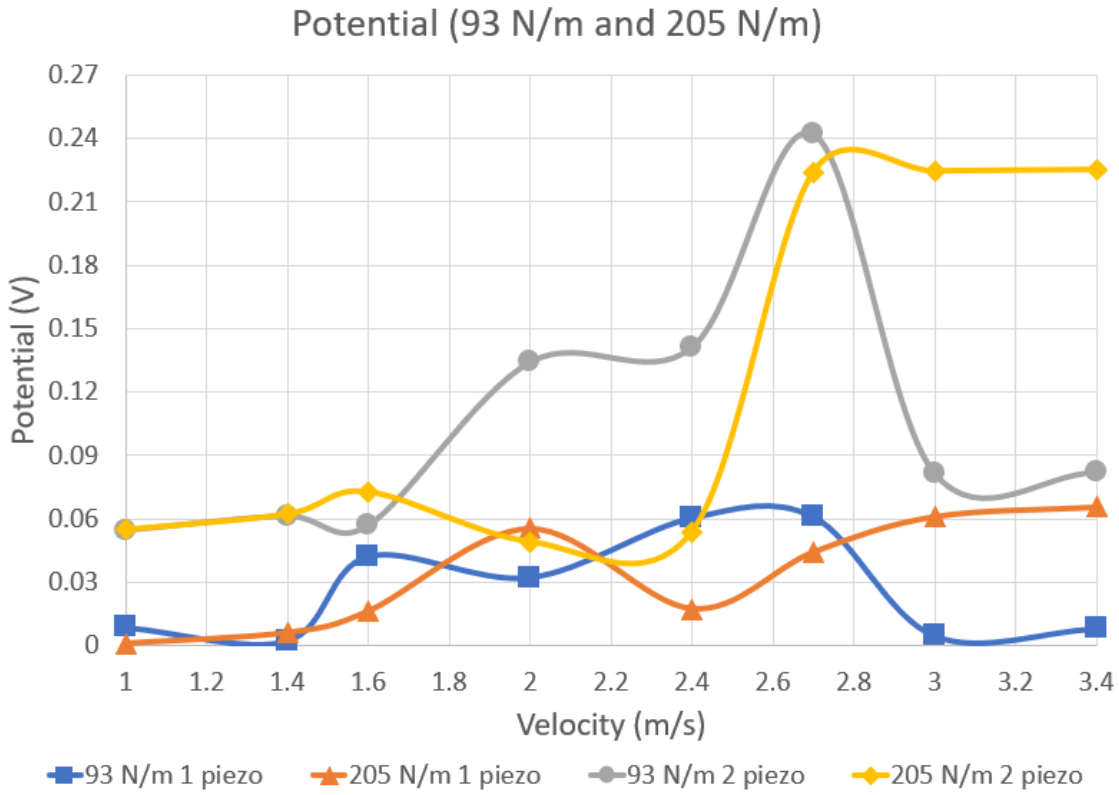

Figure 5 Behavioral Trends for potential amplitude in relation to velocity for each spring constant and number of piezoelectric transducers. This graph shows the effect of the number of piezoelectric transducers on the potential (V) of 2 springs in relation to velocity (m/s). The 2 piezoelectric transducers combination performed better than one in all scenarios for most velocities. The pattern of the potentials also slightly correlates with the spring used.

Figure 6 presents the behavior of the frequency of 4 different combinations with different spring constants and number of piezoelectric transducers with respect to velocity. Unlike **Figure 3**, the similarities between the behavior of the 2 graphs for each spring constant are less pronounced. The values for the 2 transducer graphs tended to be less than that of their counterparts. The differences between the 205 N/m combinations were well defined, but different trends were less evident with the 93 N/m spring constant. However, the differences between the frequencies are less than amplitude.

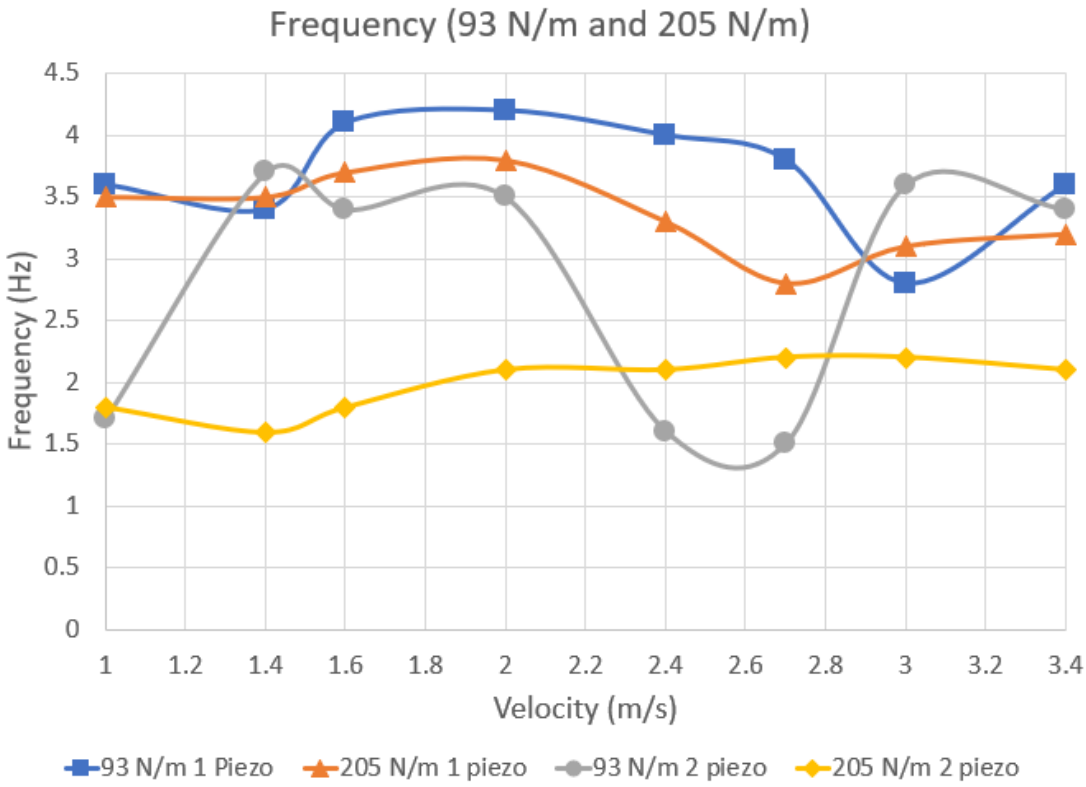

Figure 6 Behavioral trends for frequency in relation to velocity for each spring constant and number of piezoelectric transducers. This graph shows the trend in frequency for 4 combinations with different spring constants and number of piezoelectric transducers. The addition of more transducers generally decreases the frequency. However, comparison with the potential indicates a greater effectiveness of more transducers.

Tables 1a - 1d of **Appendix A** are analysis of variances done for **Tables 1 - 4**, respectively. These ANOVAs were created in order to determine if the variables involved in the research, velocity, spring constant, and the number of piezoelectric transducers, caused any significant differences between values. The p-value for the **Table 1a** did not find any significant differences between the amplitudes for all springs. However, **Tables 1b - 1d** found variables that caused significant changes. For **Table 1b**, both velocity and the spring constant were determined to be significant factors in the frequency values, since their p values of 0.034 and 0.001, respectively, were below the test value of 0.05. For **Table 1c**, only the number of piezoelectric transducers ($p = 0.001$) and velocity ($p = 0.021$) produced significant results. **Table 1d** determined that only the number of piezoelectric transducers affected the frequency, as determined by a p value of 0.002. Post hoc Holm-Sidak tests concluded that the significant differences were between the 93, 54, 314, and 636 N/m springs for frequency, and that the potentials for different numbers of piezoelectric transducers were significantly different at 1.0 and 2.7 m/s.

4. Discussion

The purpose of this phase of a larger study in vortex-induced vibration maritime engine design was to see if the use of piezoelectricity would result in a feasible design. It was believed that, if velocity was 3.4 m/s, and the generator utilized 54 N/m springs and 2 transducers, then the voltage would be the highest, and that power could operate a model ship. The research underwent 2 stages in order to determine the combination that would be the closest to achieving the highest output. However, the hypothesis cannot be supported, since the highest output achieved out of all

the combinations utilized did not occur at 3.4 m/s, 54 N/m did not achieve a high enough output to be tested with 2 transducers, and no combination achieved a high enough voltage to operate a model ship.

Analysis of the values of **Table 1** and behavior of **Figure 3** show that, if only one piezoelectric transducer is utilized, then the hypothesis would be supported. This is because the 205, 314, and 636 N/m springs achieved their highest average amplitudes at 3.4 m/s. In addition, the highest average for the one transducer combinations was achieved with the 205 N/m spring at 3.4 m/s, supporting the hypothesis. Furthermore, there exists an optimal range for the spring constants, as spring constants that were the highest or lowest did not achieve amplitudes as high as the rest of the springs. It is believed that this was the case due to the transducers adding stiffness to the bluff body, thus restricting vibration and the lock-in phenomenon, despite the presence of shedding. The restriction resulted in a shift of values, with peaks experienced in the graphs not resulting in the highest values. The results indicate the Dai et al. (2016) results would only be accurate for certain spring constants.

Table 2 and **Figure 4** show that the frequencies were not high in numerical value. As a result, the output of the entire generator was not as high as it could be with a higher frequency. The frequency was lower than was reported in previous studies because of the addition of piezoelectric transducers. These transducers reduce the freedom of vibration, thus reducing the frequency. In order to determine the springs that were to be utilized with 2 piezoelectric transducers, frequency was considered with potential. Since the 93 and 205 N/m springs achieved the highest average amplitudes for potential, and had relatively high frequencies, those springs were determined as the most effective and used in the 2-transducer testing.

Table 3 and **Figure 5** reveal that the addition of another piezoelectric transducer increased the output, and for some velocities over doubled it. This is believed to have been caused by the impact of piezoelectric transducers on the bluff body. Although the overall stiffness of the system had increased, this stiffness may have also allowed the spring and bluff body to reach resonance, thus achieving higher than expected levels of voltage. Furthermore, the utilization of a series circuit means that the highest potential was achieved from the generator. In addition, the similarities in the behaviors of the 1 and 2 transducer combinations means that the addition of more transducers is not expected to drastically alter the behavior, allowing for reasonable predictions for potential outputs, depending on the model used.

Table 4 and **Figure 6** show that the frequency was altered by the addition of another transducer. However, the decrease in frequency was less than the voltage increase, resulting in the potential compensating for the frequency. As a result, the 2 transducer combinations produced more output, regardless of a lower frequency. The behavior of **Figure 6** is notable, as the behavior of the 2 transducers graphs are not similar to those of the one transducer graphs. This could be due to slight changes in the actual vibrations of the bluff body, resulting in a complete change of behavior.

The ANOVAs were run in order to determine if differences between values did exist, as conclusions could not be made with only the descriptive data. Differences were also observed to see if the generator had to utilize one specific combination, or could use multiple combinations, which could be useful in the production and practical design of the final product. Based on the ANOVAs, there were differences in the frequencies as a result of spring constant and velocity. However, post hoc tests showed that a significant difference existed between one combination, meaning that frequencies were not significantly different and, therefore, it did not matter for the overall performance of the generator. This also holds true for the 2 transducer combinations. The results of the frequency ANOVAs are why potential was studied more than frequency in this research. Even so, the lack of significant differences in the potential for the one transducer combinations means that, theoretically, generators could utilize multiple combinations if they were to use only one transducer. However, it would still be better to use configurations that resulted in the highest output. In addition, the tests for the 2 transducer combinations showed that it was most optimal for the

generator to be running at high velocities with 2 or more piezoelectric transducers. This is because the ANOVAs indicated that the aforementioned conditions were where the greatest difference lies.

The experimentation was not completely free of issues. The construction of the structure created to support the piezoelectric transducers may have caused some form of interference with the fluid flow. This is likely due to the basic design of the generator, where the layout of the PVC pipes prevented a practical implementation of the transducers involving the structure. Furthermore, the piezoelectric transducers were determined to be too stiff, resulting in a decrease of activity in the bluff body itself. As a result, the mechanical behavior of the bluff body could not be recorded and compared to the electrical behavior. This decrease in the bluff body activity may have also resulted in lower voltage. In addition, the springs utilized in the experimentation were of different lengths, meaning that the shorter springs may have been overextended. This overextension may have resulted in different spring constants. These problems can be resolved for future work through modifications of the generator's design, such as selecting transducers with lower stiffness and replacing PVC pipes with more manipulatable objects to remove the use of a forward structure. Springs could also be selected to have the same lengths, but different spring constants. Better recording material is also being considered.

With a given current of 0.56 mA and the highest achieved voltage of 0.24 V with 2 piezoelectric transducers, the maximum power achieved from all used combinations was 0.14 MW, a value within the power range described by Jbaily and Yeung (2014), but significantly lower than the results achieved by Franzini and Bunzel (2018) and Martinez et al. (2019). Furthermore, the output would not be sufficient enough to operate a model ship, assuming that the model ship utilizes a 3.0 V motor with a current of 0.66 A, or a lithium ion battery with a potential of 3.0 V and a capacity of 0.22 Ah. Although the current configurations of the piezoelectric generator are unable to generate a sufficient amount of voltage to operate a model ship, the generator used in the experimentation was an improvement over the mechanical engine design. While the mechanical engine design was unable to produce any activity, the piezoelectric generator did manage to produce a significant output, even if the values themselves were low. It is also possible to use the current design as the basis for improvement, as adding an efficient circuit and more transducers would eventually result in a generator capable of operating a model ship. In order to achieve the target potential of 3.0 V, 24 piezoelectric transducers will be required in a circuit. However, the power produced is alternating current, resulting in the need for a bridge converter to turn the power into usable direct current power. In addition, the current from the transducers themselves are too insufficient for compatibility with the battery and motor. As a result, a step down transformer is needed to increase the current of the system. **Figure 1a** in **Appendix B** shows a circuit diagram detailing the major components of the hypothetical circuit. Although the design of the circuit in regards to the piezoelectric transducers is insignificant with the addition of a transformer, a series circuit would be preferable due to the simplicity of construction. Although it is possible to operate a model ship, scaling up to real-life dimensions presents many challenges. The results from scaling up would be unreasonable, as the piezoelectric transducer would have to be modified to accommodate a real-life ship, either by making the transducers bigger, more numerous, or more efficient. In order to confirm the capabilities of the hypothetical circuit, the current design will continue to be modified. This will be done through the actual creation of a circuit and battery to test thoughts about the final power output. The circuit itself will then be studied for its behavior and optimized to remove interfering factors. Afterwards, the battery will be added to a model ship, where the behavior of the ship will be observed in order to determine the effectiveness of the piezoelectric generator.

5. Conclusions

In this work, a vortex-induced vibration piezoelectric generator was created in order to study its merits as a source of maritime propulsion. This generator was tested using many different spring, transducer, and velocity combinations. It is determined that the hypothesis cannot be supported as the 93 N/m spring combination utilizing 2 transducers at 2.7 m/s achieved the most output of 0.24 V, not the combination predicted by the hypothesis and not enough output to power a model ship. However, the ANOVAs indicate that the generator can be greatly improved by adding at least 24 transducers in series and using the optimal combination of spring stiffness and fluid velocity. Furthermore, changes to the structural frame of the generator, decreasing the stiffness within the generator, and adding an efficient circuit could also aid in increasing the output to allow for model ship operation.

Acknowledgements

We would like to thank the Hydrogen and Fuel Cell Center at the University of South Carolina for supporting the laboratory facilities and experimental equipment for this project. We also acknowledge Spring Valley High School for providing a great opportunity to conduct this research project.

References

Dai, H. L., Abdelkefi, A., Yang, Y., & Wang, L. (2016). Orientation of bluff body for designing efficient energy harvesters from vortex-induced vibrations. *Applied Physics Letters, 108*(5), 053902. doi:10.1063/1.4941546

Franzini, G. R., & Bunzel, L. O. (2018). A numerical investigation on piezoelectric energy harvesting from vortex-induced vibrations with one and two degrees of freedom. *Journal of Fluids and Structures, 77*, 196-212. doi:10.1016/j.jfluidstructs.2017.12.007

Jbaily, A., & Yeung, R. W. (2014). Piezoelectric devices for ocean energy: A brief survey. *Journal of Ocean Engineering and Marine Energy, 1*(1), 101-118. doi:10.1007/s40722-014-0008-9

Martinez, T., Pillonnet, G., Vasic, D., & Costa, F. (2019). A longitudinal traveling wave piezoelectric transformer. *Sensors and Actuators A: Physical, 293*, 37-47. doi:10.1016/j.sna.2019.04.014

Mehmood, A., Abdelkefi, A., Hajj, M., Nayfeh, A., Akhtar, I., & Nuhait, A. (2013). Piezoelectric energy harvesting from vortex-induced vibrations of circular cylinder. *Journal of Sound and Vibration, 332*(19), 4656-4667. doi:10.1016/j.jsv.2013.03.033

Shimpalee, S. (2019). *The impact of damper properties on the amplitude and frequency of bluff body behaviors under vortex-induced vibration for maritime engines*. South Carolina Junior Academy of Science. Retrieved from https://scholarexchange.furman.edu/scjas/2019/all/273

Zhang, M., & Wang, J. (2016). Experimental study on piezoelectric energy harvesting from vortex-induced vibrations and wake-induced vibrations. *Journal of Sensors, 2016*, 1-7. doi:10.1155/2016/2673292

Appendix A

Table 1a A 2 way analysis of variance for spring constant and potential (V) of one piezoelectric transducer in relation to velocity.

Source of Variation	Difference of Squares	Sum of Squares	Mean Squares	F-test Statistic	p-value
Velocity	7	0.005670	0.000810	2.268	0.052
Spring constant	5	0.003010	0.000603	1.689	0.163
Residual	35	0.012500	0.000357		
Total	47	0.021200	0.000450		

Table 1b A 2 way analysis of variance for spring constant and frequency (Hz) of one piezoelectric transducer in relation to velocity.

Source of Variation	Difference of Squares	Sum of Squares	Mean Squares	F-test Statistic	p-value
Velocity	7	1.997000	0.285000	2.506	0.034
Spring constant	5	3.197000	0.639000	5.618	0.001
Residual	35	3.983000	0.114000		
Total	47	9.177000	0.195000		

Table 1c A 3 way analysis of variance for potential (V) of one and 2 piezoelectric transducers for 2 spring constants in relation to velocity.

Source of Variation	Difference of Squares	Sum of Squares	Mean Squares	F-test Statistic	p-value
Number of piezo	1	0.055700	0.055700	52.278	0.001
Velocity	7	0.039900	0.005700	5.350	0.021
Spring constant	1	0.000801	0.000801	0.752	0.415
Residual	7	0.007460	0.001070		
Total	31	0.147000	0.004730		

Table 1d A 3 way analysis of variance for frequency (Hz) of 1 and 2 piezoelectric transducers for 2 spring constants in relation to velocity.

Source of Variation	Difference of Squares	Sum of Squares	Mean Squares	F-test Statistic	p-value
Number of piezo	1	10.238000	10.238000	21.315	0.002
Velocity	7	2.355000	0.336000	0.700	0.675
Spring constant	1	2.588000	2.588000	5.388	0.053
Residual	7	3.362000	0.480000		
Total	31	22.837000	0.737000		

These tables show the results of the ANOVAs conducted on the research. The purpose of these ANOVAs was to determine significant variables and if any differences actually existed.

Appendix B

This diagram shows a basic outline for the parts of a hypothetical circuit. In this diagram, only a motor is shown for simplicity. The piezoelectric transducers needed to make the circuit functional is also represented by one symbol, assuming that the transducers will be in series with each other.

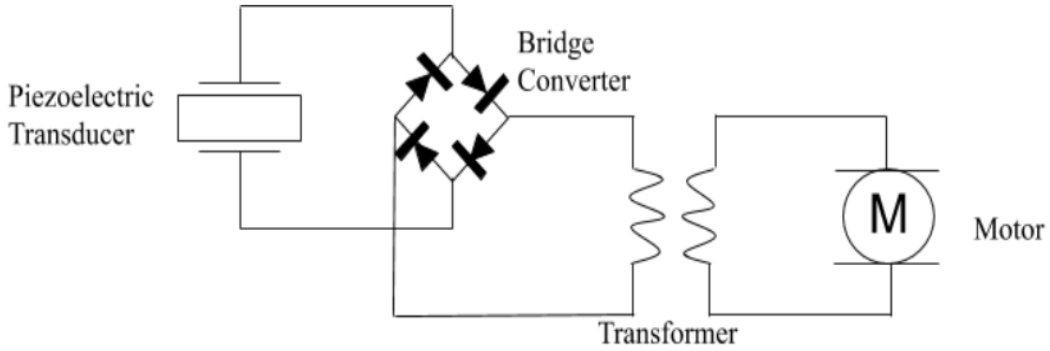

Figure 1a A circuit diagram of a hypothetical circuit utilizing the VIV-based piezoelectric generator.